Special Issue Article Open Access

Yanne K. Chembo*

Kerr optical frequency combs: theory, applications and perspectives

DOI 10.1515/nanoph-2016-0013
Received September 30, 2015; accepted January 4, 2016

Abstract: The optical frequency comb technology is one of the most important breakthrough in photonics in recent years. This concept has revolutionized the science of ultra-stable lightwave and microwave signal generation. These combs were originally generated using ultrafast mode-locked lasers, but in the past decade, a simple and elegant alternative was proposed, which consisted in pumping an ultra-high-Q optical resonator with Kerr nonlinearity using a continuous-wave laser. When optimal conditions are met, the intracavity pump photons are redistributed via four-wave mixing to the neighboring cavity modes, thereby creating the so-called Kerr optical frequency comb. Beyond being energy-efficient, conceptually simple, and structurally robust, Kerr comb generators are very compact devices (millimetric down to micrometric size) which can be integrated on a chip. They are, therefore, considered as very promising candidates to replace femtosecond mode-locked lasers for the generation of broadband and coherent optical frequency combs in the spectral domain, or equivalently, narrow optical pulses in the temporal domain. These combs are, moreover, expected to provide breakthroughs in many technological areas, such as integrated photonics, metrology, optical telecommunications, and aerospace engineering. The purpose of this review article is to present a comprehensive survey of the topic of Kerr optical frequency combs. We provide an overview of the main theoretical and experimental results that have been obtained so far. We also highlight the potential of Kerr combs for current or prospective applications, and discuss as well some of the open challenges that are to be met at the fundamental and applied level.

***Corresponding Author: Yanne K. Chembo:** FEMTO-ST Institute, CNRS & University Bourgogne Franche-Comté, Optics Department, 15B Avenue des Montboucons, 25030 Besançon cedex, France, E-mail: yanne.chembo@femto-st.fr

1 Introduction

In recent years, the topic of nonlinear phenomena in monolithic optical resonators has been the focus of a broadband interest in the scientific community. This research area has gained particular relevance owing to the new technology platforms that have allowed for the fabrication of monolithic resonators with ultra-high quality factors, such as whispering-gallery mode resonators (WGMRs) or integrated ring-resonators (RRs). These optical resonators have a size that can range from few micrometers to few millimeters, and accordingly, their free-spectral range (FSR) may vary from few terahertz to few gigahertz. From a fundamental point of view, the high-Q resonators permit to investigate various phenomena-related light-matter interactions from both the classical and quantum perspectives. From the applied viewpoint, ultra-high-Q resonators are considered as core photonic components for several microwave photonics systems. They are also considered as promising central elements for other applications such as optical filtering, add-drop systems, miniature solid-state lasers, and efficient light modulators, (see refs. [1–3] and references therein).

In these ultra-high-Q monolithic resonators, the small volume of confinement, high photon density, and long photon lifetime induce a very strong light-matter interaction (see Fig. 1), which may excite the whispering gallery modes (WGMs) through various nonlinear effects, namely, Kerr, Raman, or Brillouin. Indeed, the most interesting nonlinearity in these bulk resonators is undoubtedly induced by the Kerr effect. The Kerr effect is related to the third-order susceptibility $\chi^{(3)}$ and becomes the leading nonlinear effect in amorphous media and centrosymmetric crystals. This phenomenon originates from the quasi-instantaneous electronic response of the bulk medium to the laser excitation. When a monolithic resonator made of a Kerr-nonlinear material is pumped by a continuous-wave (CW) laser, the long-lifetime pump photons can undergo a frequency conversion and populate the neighboring eigenmodes via a degenerate four-wave mixing (FWM) interaction of the kind $2\hbar\omega_p \rightarrow \hbar\omega_i + \hbar\omega_s$, where ω_p, ω_i, and ω_s are the pump, idler, and signal angular frequencies,

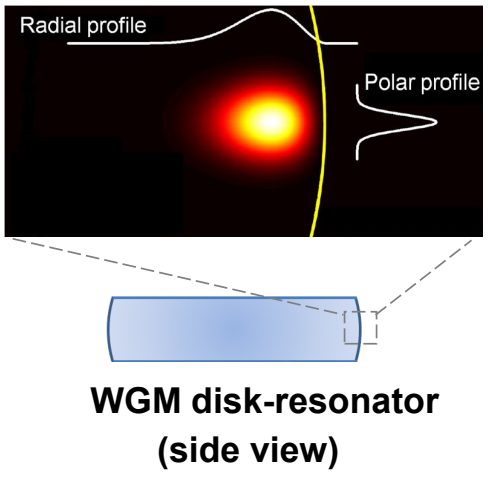

Figure 1: (Color online) Schematical representation of a torus-like eigenmode in a crystalline WGM disk-resonator (fundamental eigenmode with a single extremum in the radial and polar directions). This eigenmode can trap the intra-cavity photons for a significantly long time. Both the strong-field confinement (or equivalently, small mode volume) and the long photon lifetime (typically, $\sim$ 1 µs) contribute to enhance the nonlinear interaction between the intra-cavity photons. Such resonators typically have a Q-factor of one billion at 1550 nm.

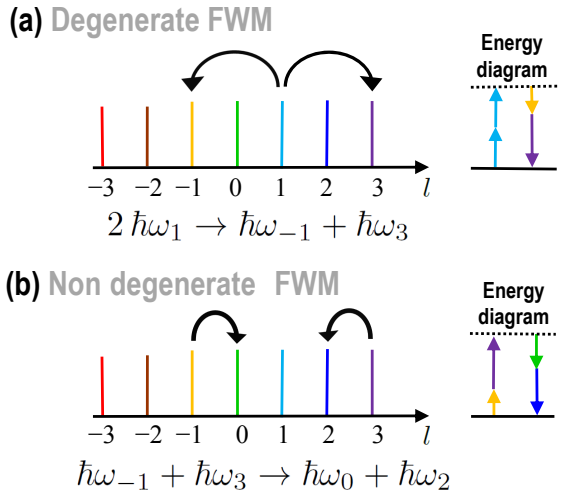

Figure 2: (Color online) Schematic representation of FWM in the frequency domain. In a given family, the eigenmodes of the resonators are quasi-equidistantly spaced as $\omega_\ell \simeq \ell\Omega_{\rm FSR}$, so that they are unambiguously labeled by their azimuthal eigenumber ℓ. It is convenient to use instead the reduced eigenumber $l = \ell - \ell_0$, with ℓ_0 being the central (pumped) mode. (a) Degenerate FWM. Two photons from one mode (not necessarily the pumped mode $l = 0$) are symmetrically up and down converted, following the interaction $2\,\hbar\omega_m \rightarrow \hbar\omega_n + \hbar\omega_q$, with $2m = n + q$. The reverse interaction $\hbar\omega_n + \hbar\omega_q \rightarrow 2\,\hbar\omega_m$ is degenerate as well. (b) Non-degenerate FWM. Two photons with eigenumbers m and p are converted into two output photons n and q through $\hbar\omega_m + \hbar\omega_p \rightarrow \hbar\omega_n + \hbar\omega_q$ where $m + p = n + q$, with the four photons being distinct.

respectively (three-mode comb), while $\hbar$ is the reduced Planck constant. The pioneering works presenting experimental evidence of this degenerate hyper-parametric oscillation were published quasi-simultaneously a decade ago by two independent research groups [4, 5]. These contributions have been followed three years later by a groundbreaking work on broadband Kerr optical frequency comb generation [6], which demonstrated that further non-degenerate interactions of the kind $\hbar\omega_m + \hbar\omega_p \rightarrow \hbar\omega_n + \hbar\omega_q$ can be triggered as well, where two input photons m and p interact coherently via the Kerr nonlinearity to yield two output photons n and q (see Fig. 2). All the excited modes are then globally coupled through FWM and, as a result, do excite an even greater number of modes, up to several hundreds. In the spectral domain, the result of this cascade of photonic interactions is generally referred to as a Kerr optical frequency comb, which can, therefore, be defined as a set of equidistant spectral components generated through the optical pumping of a monolithic resonator with Kerr nonlinearity.

The topic of Kerr combs is extremely rich and fruitful [7], as it bridges a wide range of disciplinary areas in engineering (microwave photonics, integrated photonics, metrology, aerospace and telecommunication engineering, spectroscopy, etc.), fundamental physics (crystallography, quantum optics, guided and cavity nonlinear optics, etc.), and theoretical physics (nonlinear dynamics, stochastic analysis, photonic analog computing, etc.), amongst others.

The research related to Kerr optical frequency combs is abundant and cross-disciplinary, and it intends to address different types of problems.

The first challenge has been, from the very beginning, the theoretical understanding of the Kerr comb generation process. The early models were based on a spectro-temporal (or modal expansion) approach, which used a large set of coupled nonlinear ordinary differential equations to track the individual dynamics of the excited WGMs [5, 8–11]. This formalism, where the variables are the complex-valued slowly-varying envelopes of the modal fields, has been useful, as it allowed to understand many essential features such as threshold phenomena and the role of dispersion [9]. This modal approach, however, becomes less intuitive for the theoretical analysis of the comb when the number of excited modes is large. An alternative paradigm based on a spatiotemporal approach has been introduced later on, relying on the fact that in

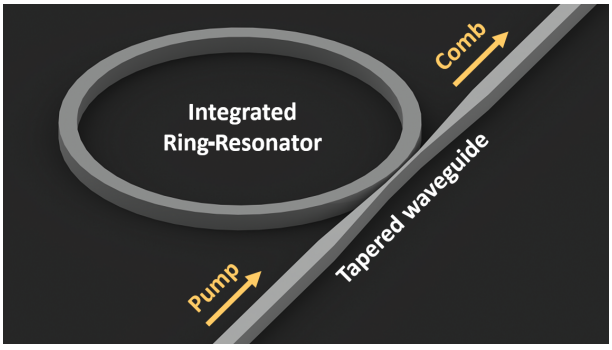

Figure 3: (Color online) An integrated ring-resonator coupled to a tapered waveguide. Such resonators typically have a Q-factor of one million at 1550 nm. The tapered section should typically be thinner than the pump wavelength in order to allow for the evanescent coupling with the resonator.

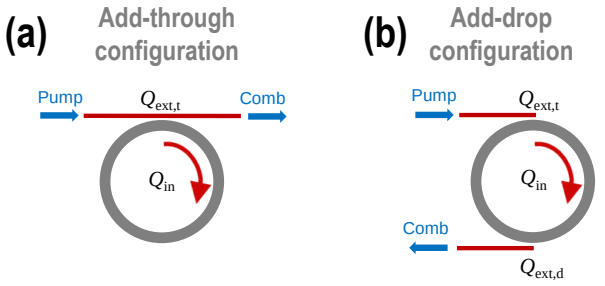

Figure 4: (Color online) The two main coupling configurations for integrated ring-resonators. The Q-factor associated to every loss mechanism is indicated in the figure (Q_{in}, $Q_{ext,t}$, and $Q_{ext,d}$ for the intrinsic, through-port, and drop-port losses, respectively). (a) Add-through coupling. Note that this nomenclature is not standard, but it is used here for being intuitive. (b) Add-drop coupling.

the resonator, light circumferentially propagates at the inner boundary of the resonator and can be treated as if it was propagating along an unfolded trajectory with periodic boundary conditions [12–15]. In this case, the overall intracavity field obeys a spatiotemporal equation referred to as the Lugiato–Lefever equation (LLE), which is a nonlinear Schrödinger equation (NLSE) with damping, detuning, and driving [16]. This LLE formalism permits to understand that Kerr combs are the spectral signature of extended or localized dissipative patterns in these optical resonators [17–19]. It was later demonstrated that the spectro- and spatiotemporal approaches are indeed equivalent and allow to understand the Kerr comb generation process from two complementary viewpoints [14].

The second challenge in the topic of Kerr combs is to generate them with the smallest energetical footprint and mass/volume payload possible. At the earliest stage, Kerr combs where predominatly investigated using tabletop experiments where such considerations where not a priority. However, as the research moved toward concrete applications, a great amount of efforts has been devoted to develop chip-scale systems with integrated RRs as in Fig. 3 [20–22], or Kerr comb generators based on crystalline WGMRs packaged in a very small volume [23]. In general, this optimization procedure particularly focuses on achieving the highest Q possible, the most efficient laser pump in coupling, as well as the highest signal-to-noise ratio for the lightwave and microwave output signals. Such optimization is critical in order to evidence the suitability of Kerr combs in comparison to existing or other prospective technologies [7].

The aim of this review article is to present a comprehensive survey of the topic of Kerr optical frequency combs. We provide an overview of the main results that have already been obtained on this topic, both at the theoretical and experimental level, and we discuss as well some of the open points that are under study in many research groups worldwide or would deserve further consideration.

The plan of the article is the following. In the next section, we present the experimental systems used for Kerr comb generation as well as the various coupling architectures used to pump the resonators and obtain a comb in the output port. Section 3 is devoted to the presentation of the two main theoretical approaches used to investigate Kerr optical frequency combs, namely, the spectro- and spatiotemporal approaches. The far-reaching implications of these two formalisms will be highlighted and discussed. The various types of combs that can be generated by pumping ultra-high-Q resonators are presented in Section 4. We show that depending on the sign of the group velocity dispersion (GVD) and on the pump power, the system can yield roll patterns, solitons, breathers, and even chaos in the spatiotemporal domain. Then, we discuss in Section 5 some of the main applications in relation with Kerr combs. Emphasis is laid on optical communications, microwave generation, spectroscopy, and quantum applications. The last section will conclude the article.

2 The experimental system

A Kerr optical frequency comb generator essentially consists in two main elements: an ultra-high-Q resonator and an input/output coupling system.

As emphasized in the introduction, the resonators can be either a WGMR or an integrated RR. They are essentially caracterized by their intrinsic quality factor Q_{in}, which can be further decomposed as $Q_{\text{in}}^{-1} = Q_{\text{vol}}^{-1} + Q_{\text{surf}}^{-1} + Q_{\text{rad}}^{-1}$, in order to account for the volumic, surface scattering, and radiation losses, respectively. The quality factor is proportional to the intrinsic photon lifetime $\tau_{\text{ph,in}}$ and inversely proportional to the full-linewidth of the resonance following $Q_{\text{in}} = \omega_0 \tau_{\text{ph,in}} = \omega_0 / \Delta\omega_{\text{in}}$, where ω_0 is the angular frequency of the mode of interest. A resonator with infinite Q would, therefore, be lossless (zero-linewidth and infinite photon lifetime).

Crystalline WGMRs tyically feature a nanometer surface roughness and very low intra-cavity losses, which allow them to reach exceptionally high-quality factors, as high as 3×10^{11} at 1550 nm [24]. The most widespread bulk materials for such resonators are fluoride crystals such as calcium fluoride [25, 26], magnesium fluoride [27, 28], lithium fluoride [29], barium fluoride [30], and strontium fluoride [31]. Ultra-high-Q resonators have also been manufactured with other materials such as fused [32, 33] and crystalline quartz [34], or even diamond [35].

On the one hand, the typical Q-factor for crystalline WGMRs is of the order of 10^9, which typically corresponds to an intrinsic photon lifetime of ∼1 μs for a resonance at ∼1550 nm. Such resonators are generally fabricated individually using a grinding and polishing technique [36]. However, it has been shown that crystalline WGMRs can be fabricated at a large scale [37] and can be integrated as well in ultra-compact devices [38].

On the other hand, integrated WGMRs and RRs typically feature a quality factor of the order of 10^6 at 1550 nm. Initially, the chip-scale resonators used for Kerr comb generation were the so-called "mushroom" WGMRs, which are toroidal resonators suspended on a pedestal. This appelation is an obvious reference to their peculiar geometrical form, and these resonators are manufactured using fused silica [6]. Later on, many research group introduced integrated RRs made of silicon nitride [20–22]. The quality factors of integrated resonators are indeed three orders of magnitude smaller than those of crystalline WGMRs, but integrated RRs still have an important advantage in comparison to WGMRs, which is their chip-scale size and structure. Generally, crystalline WGMRs are of millimeter size, yielding an FSR in the range of few gigahertz. On the other hand, because the losses in integrated resonators are dominated by the lineic absorption inside the bulk medium, they typically have a sub-millimeter size and an FSR in the terahertz range.

Beyond the intrinsic quality factor Q_{in} of the resonators, it is important to account as well for the coupling (or external) quality factor Q_{ext}. The external Q-factor can itself have several contributions depending on the actual configuration of the coupling, as shown in Fig. 4. It is noteworthy that the *add-through* configuration involves a single coupler which is used at the same time to pump the cavity and extract the comb signal in the through port with quality factor $Q_{\text{ext,t}} \equiv Q_{\text{ext}}$. Because it involves a single input/output point, this configuration allows for relatively low coupling losses, but, however, its main disadvantage is that the output signal is a superposition of the intracavity and throughtput fields [17]. The *add-drop* configuration uses one coupler to pump the resonator (quality factor $Q_{\text{ext,t}}$) and another to retrieve the comb signal at the drop port (quality factor $Q_{\text{ext,d}}$). This configuration allows to obtain an output signal that is truly proportional to the intra-cavity field, but on the other hand, it has the disadvantage to increase the coupling losses because $Q_{\text{ext}}^{-1} = Q_{\text{ext,t}}^{-1} + Q_{\text{ext,d}}^{-1}$ (see refs. [40–42]). For crystalline WGMRs, the coupling is generally performed using a tapered fiber or a prism coupling. The first solution is the most energetically efficient because it allows for coupling efficiencies above 99%, while the second one is more robust, still with a coupling efficiency as high as 70%. On the other hand, integrated RRs almost exclusively use the tapered waveguide technique. Other options are of course possible, such as tapered fiber coupling for chip-scale mushroom resonators or angle-polished coupling for WGMRs.

The dynamics of the intracavity field will essentially be ruled by the total quality factor $Q_{\text{tot}}^{-1} = Q_{\text{in}}^{-1} + Q_{\text{ext}}^{-1}$, to which an overall photon lifetime and resonance linewidth can be associated through $Q_{\text{tot}} = \omega_0 \tau_{\text{ph}} = \omega_0 / \Delta\omega_{\text{tot}}$. Since this total quality factor is necessarily smaller than both Q_{in} and Q_{ext}, it is important to optimize the coupling factor as well in order to obtain an overall quality factor that is still ultra-high. The resonator is considered under-coupled when $Q_{\text{in}} < Q_{\text{ext}}$, over-coupled when $Q_{\text{in}} > Q_{\text{ext}}$, and critically coupled when $Q_{\text{in}} = Q_{\text{ext}}$. These quality factors can be experimentally determined using the cavity-ring down method [39].

The main motivation for achieving ultra-high Q factors is that it permits to trigger Kerr combs with smaller pump powers. More specifically, the threshold pump power to obtain a Kerr comb scales as $1/Q_{\text{tot}}^2$, as it will be shown in the next section. It should also be noted that the choice of the optimal coupling architecture (add-through or add-drop), quality factors (under-, critical, over-coupling), and coupling system (prism, taper, etc.) ultimately depends on the final application for the output Kerr comb.

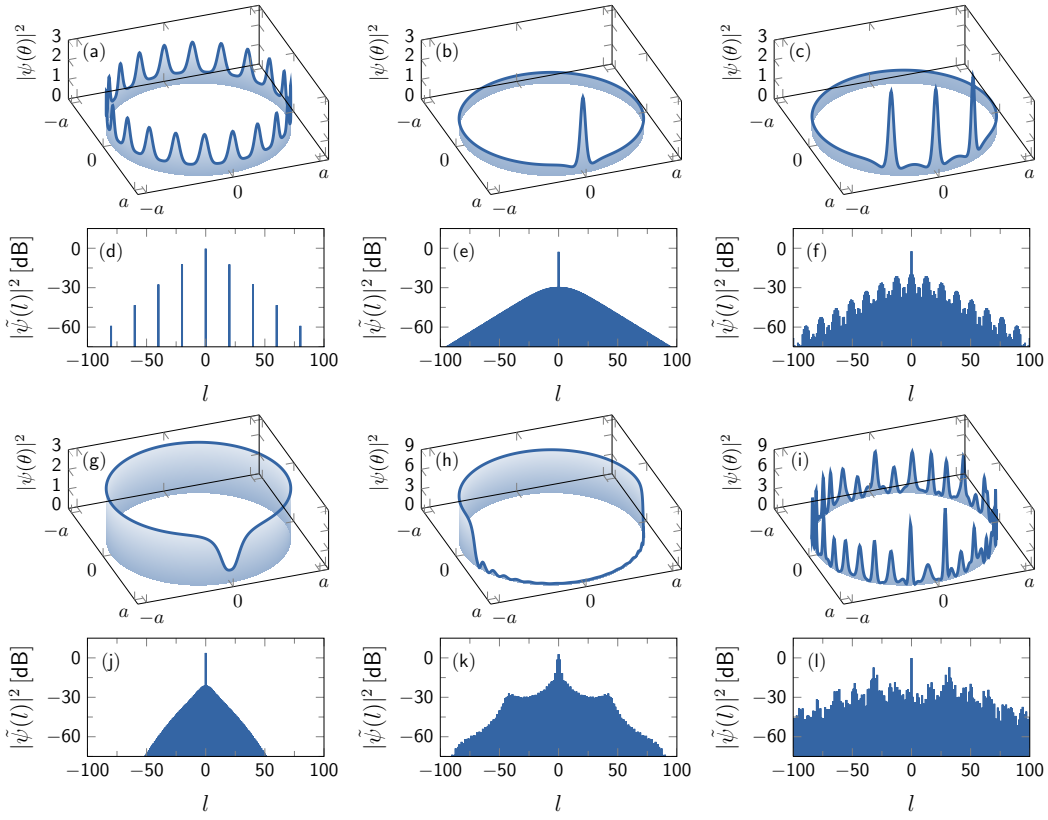

Figure 5: (Color online) Various spatiotemporal solutions and their corresponding spectra (Kerr combs), obtained after simulation of Eq. (3). The conditions under which these solutions can be excited are investigated in detail in ref. [18]. For all these simulations, we consider a CaF_2 resonator coupled in the add-through configuration, with $a = 2.5$ mm, $\lambda_L = 1550$ nm, $Q_{int} = 4Q_{ext} = 10^9$, $n_g = 1.43$, $g_0 = 2\pi \times 60$ μHz, and a free-spectral range $\Omega_{FSR}/2\pi = 13.35$ GHz. The absolute value of the GVD is set to $|\zeta_2| = 2\pi \times 2.9$ kHz for both anomalous and normal GVD. Note that the pumped mode is $l = 0$, so that the sidemodes expand as $l = \pm1, \pm2, \ldots$ (a) and (d) Roll pattern of order $L = 20$ ($P = 2.5$ mW and $\sigma = -\Delta\omega_{tot}/2$). (b) and (e) Bright soliton ($P = 3.5$ mW and $\sigma = -\Delta\omega_{tot}$). (c) and (f) Bright soliton molecule ($P = 3.5$ mW and $\sigma = -\Delta\omega_{tot}$); (g) and (j): Dark soliton ($P = 5.3$ mW and $\sigma = -1.25\,\Delta\omega_{tot}$), (h) and (k): Platicon ($P = 17.3$ mW and $\sigma = -3\,\Delta\omega_{tot}$). (i) and (l): Chaos ($P = 15$ mW and $\sigma = -\Delta\omega_{tot}/2$).

3 Modeling Kerr combs

WGMs and RRs are characterized by several geometrical and material properties that have to be accounted for in order to achieve an accurate modelling of Kerr optical frequency comb generation.

Generally, the resonators can host a very large set of eigenmodes families, defined by their radial and polar eigenumbers. However, the theoretical understanding of Kerr combs only requires to consider a single family (with fixed polar and radial eigenumbers) containing a large number of torus-like azimuthal modes [1–3]. Within the eigenmode family under study, the modes of interest are unambiguously defined by a single integer wavenumber ℓ, which can be interpreted as the mode's angular momentum or, equivalently, the total number of reflections that a photon in this mode undergoes during one round trip in the cavity in the ray-optics interpretation. If we consider that the eigennumber of the pumped is ℓ_0 and its frequency is ω_{ℓ_0}, it is convenient to introduce the reduced eigenumber $l = \ell_0 - \ell$ which is such that the pumped mode is $l = 0$, while the sidemodes symmetrically expand as $l = \pm1, \pm2, \ldots$ with "+" and "–" standing, respectively, for higher and lower frequency sidemodes.

The spectral distance $\omega_{l+1} - \omega_l$ between two consecutive modes is referred to as the FSR and for a resonator with closed-path perimeter L, the FSR can be explicitly determined as $F_{FSR} = c/n_g L = v_g/L$, where c is the velocity of light in vacuum, n_g is the group-velocity refraction index at ω_l, and v_g is the corresponding group velocity. It should be noted that the FSR is linked to the round-trip period along the perimeter of the resonator following $T_{FSR} = 1/F_{FSR}$.

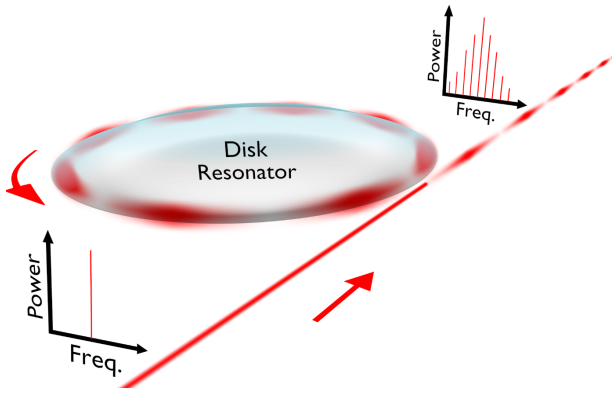

Figure 6: Schematic representation of Kerr optical frequency comb generation using a crystalline disk resonator. In this figure, we consider the case where a continuous-wave input pump creates a roll pattern (eighth order) inside the disk resonator, which induces a a periodic intensity modulation along the rim. The output signal spectrally corresponds to an optical frequency comb with extremely high coherence and robustness, featuring an eight-FSR spacing. Depending on the laser pump power and frequency, many other stationary (solitons) and non-stationary (chaos, breathers) spatiotemporal patterns can be excited inside the nonlinear resonator, as shown in Fig. 5.

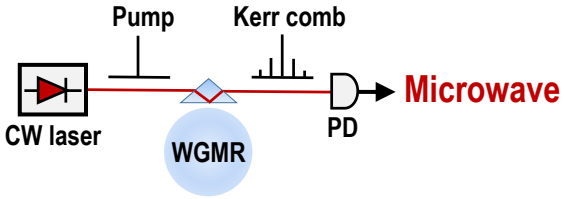

Figure 7: Simplified experimental set-up for microwave generation using Kerr combs. CW, continuous wave; PD, photodetector. The very high spectral requirement justifies the utilization of crystalline WGM Rs with billion quality factor at 1550 nm. The prism is the preferred coupling solution in this case for the sake of improved robustness. A stationary and coherent Kerr comb would yield an ultra-pure microwave after photodetection.

The eigenmodes ω_l are in fact not strictly equidistant. The measure of this nonequidistance is referred to as overall dispersion, which explicitly appears when the eigenfrequencies of the resonator are Taylor expanded around the pumped mode following $\omega_l = \omega_0 + \sum_{k=1}^{k_{\max}} (\zeta_k/k!)\, l^k$, where $k_{\max}$ is the order of truncation, $\zeta_1 \equiv 2\pi F_{\text{FSR}} = \Omega_{\text{FSR}}$ is angular frequency FSR, ζ_2 represents the second-order GVD, and ζ_k for $k \geq 3$ corresponds to higher-dispersion terms. Note that perfect equidistance for the eigenfrequencies would be achieved by setting the dispersion to zero, that is, $\zeta_k \equiv 0$ for all $k \geq 2$. It is important to note that dispersion has a geometrical and a material contribution.

Another parameter of interest is the effective mode volume V_{eff}, or equivalently, the effective mode area $A_{\text{eff}} = V_{\text{eff}}/L$, of the torus-like eigenmodes within which the intra-cavity photons are trapped. The smallest mode areas induce a stronger confinement of the intracavity photons. Strictly speaking, the mode volume does vary weakly as a function of the eigenmode order l, but for sake of simplicity, we will consider here that these parameters are degenerated and, therefore, equal for all the modes under consideration.

Kerr comb generation is actually mediated by the Kerr nonlinearity that induces a dependence of the refraction index with regards to the intracavity electric field following $n = n_0 + n_2 I$, where n_0 is the refraction index at the frequency ω_0, n_2 is the Kerr coefficient, and I is the irradiance of the field (proportionnal to its square modulus). In the studies led with a cavity electrodynamics mindset, the intracavity fields are evaluated in terms of number of photons and the Kerr nonlinearity is generally accounted for through the FWM gain $g_0 = n_2 c\hbar\omega_0^2/n_0^2 V_{\text{eff}}$ (in rad/s). On the other hand, in research works undertaken with a nonlinear optics approach, the power of intracavity fields is measured in watts and the Kerr nonlinearity is accounted for through the coefficient $\gamma = \omega_0 n_2/cA_{\text{eff}}$ in $\text{W}^{-1}\text{m}^{-1}$, which is, for example, extensively used in fiber optics research [43].

Using the above parameters, Kerr optical frequency comb dynamics can be modelized using two complementary approaches, namely, a spectrotemporal approach using coupled-mode equations (CME), and a spatiotemporal approach using the LLE. These approaches aim to describe the dynamics of the complex-valued, slowly-varying envelopes of the intra-cavity fields. They are valid as long as the temporal dynamics of these fields is typicaly slower than the round-trip period of the resonator. Both formalisms can also be translated into the quantum realm and yield quantum Langevin equations (QLE). These theoretical approaches are reviewed hereafter.

3.1 Spectrotemporal model: coupled-mode equations (CME)

The first type of models that have been proposed to investigate the dynamics of Kerr combs are spectrotemporal models, which are also sometimes referred to as modal-expansion or coupled-mode models. This approach was initially developped in [5] for the case of pump, signal and idler dynamics. It was later on generalized in ref. [9] to account for an arbitrary number of modes. The main idea of

this approach is that the optical field of each mode can be described by its complex-valued slowly-varying envelope $\mathcal{A}_l$. Therefore, a set of coupled equations can be established to describe the dynamics of each amplitude $\mathcal{A}_l$ as a function of losses, dispersion, nonlinearity, as well as the laser pump and frequency.

It can be demonstrated that the modal fields $\mathcal{A}_l$ obey the following set of autonomous, nonlinear, and coupled ordinary differential equations (see ref. [9]):

$$\begin{aligned}\dot{\mathcal{A}}_l &= -\frac{1}{2}\Delta\omega_{\rm tot}\,\mathcal{A}_l + i\left[\sigma - \sum_{k=2}^{k_{\rm max}} \frac{\zeta_k}{k!}\, l^k\right] \mathcal{A}_l \\ &\quad + ig_0 \sum_{m,n,p} \delta(m-n+p-l)\,\mathcal{A}_m \mathcal{A}_n^* \mathcal{A}_p \\ &\quad + \delta(l)\sqrt{\Delta\omega_{\rm ext,t}}\,A_{\rm in}\,, \end{aligned} \tag{1}$$

where the overdot indicates the time derivative, and $\delta(x)$ is the Kronecker delta function that equals 1 when $x = 0$ and equals zero otherwise. In the above equation, the Kronecker function indicates that only the mode $l = 0$ is pumped, and that the allowed FWM interactions will be those for which the total angular momentum of the interacting photons is conserved, following $m + p = n + l$. An important parameter of the above equation is the detuning parameter $\sigma = \omega_{\rm L} - \omega_0$, which is the difference between the angular frequencies of the laser of power P (in watts) and of the pumped mode resonance. The term standing for the pump field is $A_{\rm in} = \sqrt{P/\hbar\omega_{\rm L}}$, and it corresponds to the square root of the input photon flux. The above model also assumes several simplifications, such as spatial degeneracy (all the eigenmodes are perfectly overlapped spatially) and loss degeneracy (all the modes have the same loss coefficients).

In the above equation, the frequency reference is set at the laser frequency and the slowly-varying amplitudes $\mathcal{A}_l$ are defined with respect to the equidistant grid of eigenmodes, while in the original model of ref. [9], the frequency reference is set at the pumped resonance frequency, and the sidemodes are defined with respect to the dispersion-detuned eigenfrequency grid. Equation (1) has also been complex conjugated with respect to the original modal expansion model (see [9, 18]). It is also important to recall that the fields in Eq. (1) are normalized such that $|\mathcal{A}_l|^2$ is a number of photons (dimensionless).

3.2 Spatiotemporal model: the Lugiato–Lefever equation (LLE)

The complementary approach to the spectrotemporal model is the spatiotemporal approach, where instead of tracking the time-domain dynamics of individual modes $\mathcal{A}_l(t)$, we follow the spatiotemporal dynamics of the total intracavity field $\mathcal{A}(\theta, t) = \sum_l \mathcal{A}_l(t) e^{il\theta}$, where $\theta \in [-\pi, \pi]$ is the azimuthal angle along the closed-path circumference of the resonator. It has been shown in refs. [13–15] that the total intracavity field $\mathcal{A}(\theta, t)$ obeys a nonlinear partial differential equation which is generally referred to as the Lugiato–Lefever equation (LLE). The LLE was initially introduced by Lugiato and Lefever almost 30 years ago as a paradigmatic equation for the understanding of self-organization and dissipative structures in nonlinear optics [16]. In the case of Kerr combs, it has been shown in ref. [14] that the above modal expansion model is exactly equivalent to the following generalized LLE in the moving frame

$$\begin{aligned}\frac{\partial \mathcal{A}}{\partial t} &= -\frac{1}{2}\Delta\omega_{\rm tot}\,\mathcal{A} + i\sigma\mathcal{A} + iv_g \sum_{k=2}^{k_{\rm max}} (i\Omega_{\rm FSR})^k \frac{\beta_k}{k!}\frac{\partial \mathcal{A}}{\partial \theta^k} \\ &\quad + ig_0|\mathcal{A}|^2\mathcal{A} + \sqrt{\Delta\omega_{\rm ext,t}}\,A_{\rm in}\,, \end{aligned} \tag{2}$$

where the new dispersion coefficients $\beta_k = -[v_g(-\Omega_{\rm FSR})^k]^{-1}\,\zeta_k$ exactly correspond to those generally used in fiber optics research.

Equation (2) is a nonlinear partial differential equation with periodic boundary conditions. For that reason, the numerical simulations of the LLE are optimally performed using the split-step Fourier algorithm, which is a particularly efficient algorithm that inherently assumes such periodic boundary conditions because it is based on the fast Fourier transform (FFT). As a technical note, several authors write the LLE with two timescales, and this particular approach finds its origin in earlier works performed in the context of nonlinear fiber ring cavities [44, 45]. However, this two timescales LLE is strictly equivalent to the spatiotemporal LLE of Eq. (2), which follows the viewpoint of cavity nonlinear optics. The spatiotemporal formulation appears to be the most logical in the context of Kerr combs because the azimuthal angle θ is intrinsically a periodic variable that inherently respects the physical nature of the boundary conditions and also because l and θ are natural conjugate variables from the Fourier analysis standpoint.

The output fields can explicitly be expressed as $\mathcal{A}_{\rm out} = \sqrt{\Delta\omega_{\rm ext,t}}\,\mathcal{A} - A_{\rm in}$ in the add-through configuration and as $\mathcal{A}_{\rm out} = \sqrt{\Delta\omega_{\rm ext,d}}\,\mathcal{A}$ in the add-drop configuration [40]. It is also useful to note that the intracavity and output fields $\mathcal{A}$ and $\mathcal{A}_{\rm out}$ can be, respectively, rescaled to $\mathcal{E} = \sqrt{\hbar\Omega_{\rm L}/T_{\rm FSR}}\,\mathcal{A}$ and $\mathcal{E}_{\rm out} = \sqrt{\hbar\Omega_{\rm L}}\,\mathcal{A}_{\rm out}$, which have a square modulus in units of watts.

Most studies restrict their analysis to the case where higher-order dispersion is neglected ($\beta_k \equiv 0$ for $k \geq 3$). In

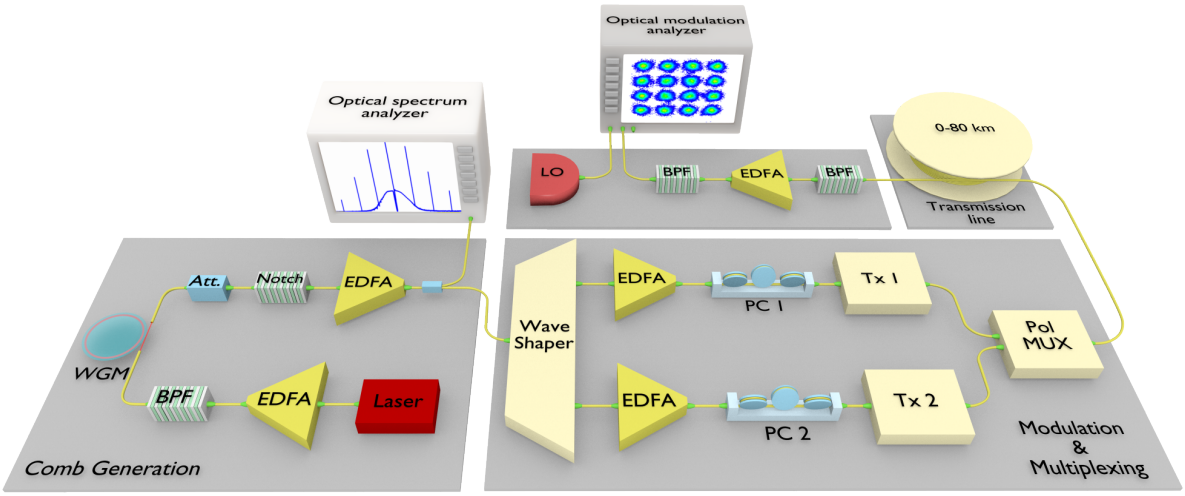

Figure 8: (Color online) Schematic representation of the experimental setup for ultra-high capacity optical coherent telecommunications. A Kerr comb is used as a multi-wavelength coherent source fo WDM optical telecommunications. EDFA, erbium-doped fiber amplifier; BPF, bandpass filter; PC, polarization controllers; PolMUX, polarization multiplexing; LO, local oscillator. The signal of a CW laser is first amplified and filtered to reject the EDFA noise. This signal is used to pump an ultra-high-Q WGMR, and a coherent Kerr comb (primary comb corresponding to a roll patern) is obtained at the output port. This comb is amplified, and a notch filter attenuates the center mode to a level comparable to the first-order side modes of the comb. A programmable filter is used for interleaving, flattening, and filtering the comb lines. Two EDFAs boost the carriers, which are fed via polarization controllers to two transmiters. The data streams are then multiplexed, mergedand, launched in the transmission fiber. At the receiver end, the data streams are band-pass filtered and amplified before being coherently detected with an external cavity laser serving as a local oscillator. The received data are visualized using constellation diagrams that display the real and the imaginary part of the optical amplitude in the complex plane. This experiment enabled to transmit data at up to 144 Gbit/s per carrier.

that case, the above equation can be simplified and normalized as

$$\frac{\partial \psi}{\partial \tau} = -(1 + i\alpha)\psi - i\frac{\beta}{2}\frac{\partial^2 \psi}{\partial \theta^2} + i|\psi|^2\psi + F, \qquad (3)$$

where $\psi(\theta, \tau) = (2g_0/\Delta\omega_{\text{tot}})^{1/2}\mathcal{A}(\theta, \tau)$ is the total intracavity field, $\tau = \Delta\omega_{\text{tot}}t/2 = t/2\tau_{\text{ph}}$ is the dimensionless time, $\alpha = -2\sigma/\Delta\omega_{\text{tot}}$ is the cavity detuning, and $\beta = -2\zeta_2/\Delta\omega_{\text{tot}}$ is the second-order GVD (defined as normal for $\beta > 0$ and anomalous for $\beta < 0$). The driving term of the normalized LLE is $F = (8g_0\Delta\omega_{\text{ext,t}}/\Delta\omega_{\text{tot}}^3)^{1/2}\sqrt{P/\hbar\Omega_0}$ and stands for the external pump excitation. From the mathematical point of view, Eq. (3) exactly corresponds to the original equation introduced by Lugiato and Lefever in ref. [16]. However, it is interesting to note that in the original LLE, the Laplacian term stands for diffraction instead of dispersion in the case of Kerr comb generation.

3.3 Quantum Langevin equations (QLE)

As Kerr optical frequency combs result from a cascade of photonic interactions involving individual photons, purely quantum phenomena based on the nonclassical nature of light can play a significant role in these combs [46]. The dynamics of Kerr optical frequency combs at the quantum level is determined using an Hamiltonian operator (which has the advantage to be helpful for the determination of conservation rules) or using the canonical quantization (which has the advantage to be more intuitive).

On the one hand, the quantum state of each mode l can be described by the annihilation and creation operators $\hat{a}_l$ and $\hat{a}_l^\dagger$, which are the quantum counterparts of the slowly varying envelopes $\mathcal{A}_l$ and $\mathcal{A}_l^\star$, respectively. These operators are Hermitian conjugates of each other, and they obey the boson commutation rules $[\hat{a}_l\,, \hat{a}_{l'}^\dagger] = \delta_{l,l'}$ and $[\hat{a}_l, \hat{a}_{l'}] = [\hat{a}_l^\dagger, \hat{a}_{l'}^\dagger] = 0$. On the other hand, the semiclassical photon number $N_l = |\mathcal{A}_l|^2 = \mathcal{A}_l^\star\mathcal{A}_l$ should now be replaced by its quantum counterpart, which is the photon number operator $\hat{n}_l = \hat{a}_l^\dagger\hat{a}_l$.

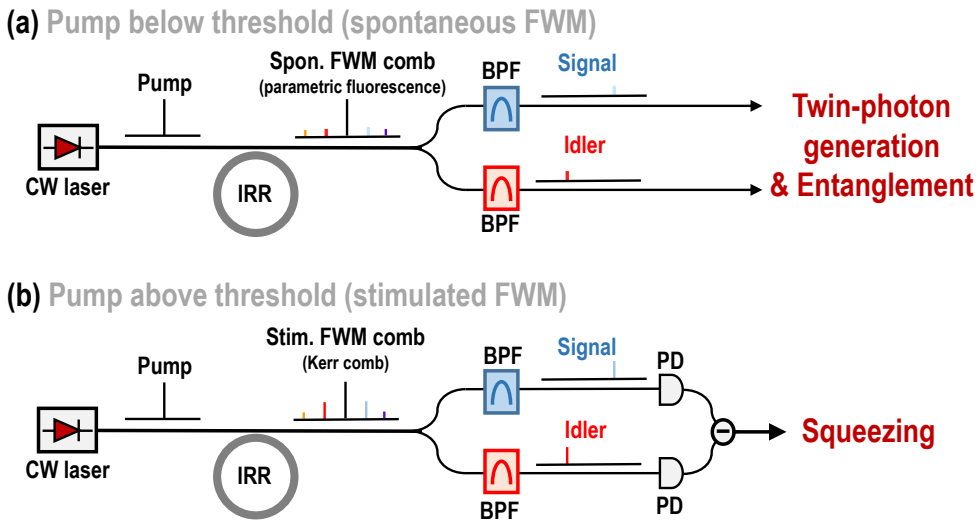

Figure 9: (Color online) Simplified experimental setups for the analysis of the quantum states of Kerr combs. (a) Pump below threshold. The setup allows to investigate parametric fluorescence and entangled photon pair generation. (b) Pump above threshold. The setup permits to investigate quantum correlations and two-mode squeezing.

In the Heisenberg picture, quantum Kerr combs can be described by the following set of differential equations

$$\begin{aligned}\dot{\hat{a}}_l = &-\frac{1}{2}\Delta\omega_{\rm tot}\,\hat{a}_l + i\left[\sigma - \sum_{k=2}^{k_{\rm max}}\frac{\zeta_k}{k!}\,l^k\right]\hat{a}_l \\ &+ ig_0\sum_{m,n,p}\delta(m-n+p-l)\,\hat{a}_n^\dagger\hat{a}_m\hat{a}_p \\ &+ \delta(l)\,\sqrt{\Delta\omega_{\rm ext,t}}\,A_{\rm in} + \sum_{\rm s}\sqrt{\Delta\omega_{\rm s}}\,\hat{V}_{{\rm s},l}\,, \qquad (4)\end{aligned}$$

where $\hat{V}_{{\rm s},l}(t)$ is the vacuum fluctuation operator that have to be associated to every loss mechanism for each mode l, with s being an index running across the various loss terms corresponding to the configuration under study (intrinsic, through-port, and eventually drop-port). These vacuum fluctuation operators have zero expectation value and obey the commutation rules $[\hat{V}_{{\rm s},l}(t), \hat{V}^\dagger_{{\rm s}',l'}(t')] = \delta_{{\rm s},{\rm s}'}\,\delta_{l,l'}\,\delta(t-t')$.

The annihilation operator of the total intracavity field can also be described by the operator $\hat{a}(\theta,t) = \sum_l \hat{a}_l(t)\,e^{il\theta}$ that obeys the quantum LLE

$$\begin{aligned}\frac{\partial\hat{a}}{\partial t} = &-\frac{1}{2}\Delta\omega_{\rm tot}\,\hat{a} + i\sigma\hat{a} + iv_g\sum_{k=2}^{k_{\rm max}}(i\Omega_{\rm FSR})^k\frac{\beta_k}{k!}\frac{\partial^k\hat{a}}{\partial\theta^k} \qquad (5)\\ &+ ig_0\,\hat{a}^\dagger\hat{a}^2 + \sqrt{\Delta\omega_{\rm ext,t}}\,A_{\rm in} + \sum_{\rm s}\sqrt{\Delta\omega_{\rm s}}\,\hat{V}_{\rm s},\end{aligned}$$

where $\hat{V}_{\rm s}(\theta,t) = \sum_l \hat{V}_{{\rm s},l}(t)\,e^{il\theta}$.

The above QLE permit the quantum analysis of Kerr combs when the resonators are pumped below and above threshold, thereby allowing for the understanding of phenomena such as entanglement, spontaneous FWM, or two-mode squeezing [46].

4 Various types of solutions and their corresponding spectra

We present here the main types of Kerr optical frequency combs that can be obtained both experimentally and theoretically. We classify these combs using the dynamical characteristics of their spatiotemporal waveform, which is indeed associated to a particular kind of Kerr comb in the spectral domain. In this review, we restrict the analysis to the case where only the second-order dispersion is accounted for, so that the system can be analyzed using the normalized LLE of Eq. (3). It can be shown that the types of solutions and their basin of attraction strongly depend on the dispersion regime [18]. In the anomalous dispersion regime, the stationary solutions are rolls (super- and subcritical), bright solitons (isolated or coexisting), and soliton molecules (isolated or coexisting). In the case of normal dispersion, the stationary solutions can be rolls, dark solitons (isolated or coexisting), and breathers. Figure 5 displays the various types of solutions that are generally obtained in both the spatial and spectral domains. The dynamical nature of these solutions is explained in the following sub-sections.

4.1 Rolls

Roll patterns emerge from noise after the breakdown of an unstable flat background through modulational instability, when the resonator is pumped above a certain threshold. This mechanism preferably occurs in the regime of anomalous GVD, but, however, rolls can also be sustained in the normal GVD regime, although under very marginal conditions (typically, very large detuning, see refs. [9, 18, 47]).

When the pump is below the threshold, there is only one excited mode in the resonator ($l = 0$), while all the sidemodes amplitudes $\mathcal{A}_l$ with $l \neq 0$ are null. From the spatiotemporal standpoint, the intracavity field is constant (flat background). Under certain conditions, when the pump F is increased beyond a certain threshold value F_{th}, the flat background solution becomes unstable and breaks down into a roll pattern characterized by a periodic modulation of the intracavity power as a function of the azimuthal angle (see Fig. 6). This phenomenology is generally referred to as *modulational instability* in nonlinear optics, and as the *Benjamin–Feir instability* in fluid mechanics. As a historical note, this kind of instability has in fact been foreshadowed for the first time by Alan Turing in his seminal work on the chemical basis of morphogenesis. His toy model was a "*continuous ring of tissue,*" and his main finding was that "*in the most interesting form stationary waves appear on the ring*" [48]. The work of Turing became a paradigm for reaction–diffusion systems, and in that context, the modulational instability is also sometimes referred to as the *Turing bifurcation*.

It has been demonstrated that the number of rolls that appear in the azimuthal direction when the cavity is pumped just above the threshold of modulational instability is equal to the closest integer approximation of $l_{\text{th}} = [2\,|(\alpha - 2)/\beta|]^{\frac{1}{2}} = [2\,|(\sigma + \Delta\omega_{\text{tot}})/\zeta_2|]^{\frac{1}{2}}$. In the spectral domain, the Kerr comb corresponding to this roll pattern will feature a multiple-FSR spacing, with a multiplicity exactly equal to l_{th}, and they are sometimes referred to as *primary combs* [9].

It is also noteworthy that roll patterns can emerge following either a supercritical bifurcation (soft excitation) or a subcritical bifurcation (hard excitation), as already emphasized in the original work of Lugiato and Lefever [16]. On the one hand, supercritical bifurcations to roll patterns occur when $\alpha < 41/30$ in the anomalous GVD regime, and they correspond to the case where the roll pattern ($F > F_{\text{th}}$) cannot coexist with the flat background ($F < F_{\text{th}}$). On the other hand, still for anomalous GVD, subcritical bifurcations arise when $\alpha > 41/30$. Here we still have a roll pattern beyond F_{th} and a flat background below F_{th}, but, however, there is a small range below F_{th} where both the flat solution and the roll pattern are stable and coexist. This area of bistability also displays hysteresis, so that the asymptotic solution depends on the initial condition, and external perturbations can switch the system from one solution to another [18].

At the experimental level, primary combs have been evidenced for the first time in ref. [25], and since then, they have been reported and investigated in numerous studies (see, e.g., ref. [17]). These particular Kerr comb spectra are characterized by a very strong mode locking [49], particularly in the supercritical case with low l_{th} and just above threshold, where the roll pattern is the only stable solution. It should also be noted that experimentally, primary combs with a multiplicity higher than 200 have already been demonstrated [50], and this multiplicity typically increases as $|\beta| \to 0$.

It has also been shown that the absolute minimum pump power to excite a roll pattern in a resonator of radius a is

$$P_{\text{min}} = \frac{\hbar\omega_{\text{L}}}{8g_0}\frac{\Delta\omega_{\text{tot}}^3}{\Delta\omega_{\text{ext,t}}} = 2\pi a\,\frac{\omega_{\text{L}}^2}{8\gamma v_g^2}\frac{Q_{\text{ext,t}}}{Q_{\text{tot}}^3}\,. \tag{6}$$

Therefore, a millimeter-sized crystalline resonator with billion quality factor at 1550 nm would have a threshold power of the order of few milliwatt, while a sub-millimeter integrated silicon nitride resonator with million quality factor would rather have a threshold power of a watt. It can also be demonstrated that P_{min}, which is proportional to V_{eff}/Q^2, is with an excellent approximation the absolute minimum value needed to excite any type of comb.

4.2 Bright, dark, and breather solitons

In general, conservative solitons result from the balance between nonlinearity and dispersion, which defines their shape. In dissipative cavities, it is necessary to achieve as well the balance between gain and dissipation, which defines their amplitude. At the opposite of rolls that are *extended* dissipative patterns, cavity solitons are *localized* dissipative structures that are coexisting with one or two stable flat background solutions.

Bright solitons are by essence subcritical, because they correspond to a pulse that has been isolated from a subcritical roll pattern in the anomalous dispersion regime [18]. In the spectral domain, Kerr combs corresponding to solitons display up to several hundred phase-locked modes, with a number of modes that increases as $|\beta| \to 0$. Depending on the initial conditions (i.e., on how the system is excited from a flat background state),

multipeaked solutions, which are referred to as *soliton molecules*, can emerge in the system. The number of peaks actually depends on the initial conditions and can be interpreted as a set of contiguous pulses that have been carved out of a subcritical roll pattern. The bright solitons have also been observed in recent experiments [51], and different strategies have been proposed to excite them [52].

Dark solitons are localized structures that are characterized by a "hole" in a flat background. These solitons coexist with two stable flat solutions (sometimes referred to as "up" and "down" solutions) and particular initial conditions are needed to excite them. The dark solitons can be a dip in the background or can feature a large depression (and be referred to as a *platicon* [53]), depending on the parameters of the system.

Under certain conditions, the solitons might lose their stability and bifurcate to breathers, which are solitons whose amplitude varies periodically in time. The breathing period is typically very low and remains of the order of the photon lifetime. These breathers naturally lead to nonstationary Kerr combs.

The bright, dark, and breather cavity solitons are localized dissipative structures, and they are not influenced by the boundary conditions as long as their typical linewidth is smaller than the closed-path perimeter of the resonator. It is, therefore, possible to excite simultaneously several solitons of the same type inside the resonator, and they remain uncoupled as long as their linewith remains much smaller than the distance between them.

4.3 Chaos

A system is considered chaotic when it is deterministic, unpredictable, and sensitive to initial conditions. It is known that the necessary (but not sufficient) conditions for the emergence of chaos are nonlinearity and three-fold dimensionality in the state space. A third condition, which is rather empirical but intuitively evident, is the requirement of "strong" excitation. The equations ruling the dynamics of Kerr combs (LLE or CME) can fulfill all these conditions and therefore predict the occurence of spatiotemporal chaos. The first unambigous evidence of spatiotemporal chaos in Kerr combs was provided in ref. [8] using the computation of Lyapunov exponents, which were found to be positive in the case of strong pumping. Other studies such as ref. [54] have also shed more light on the chaotic dynamics of Kerr combs.

From a more general perspective, two main routes to chaos can be identified for Kerr combs [55]. The first route corresponds to the destabilization of roll patterns. In that case, the rolls start to oscillate chaotically and in the spectral domain, the Kerr comb features very strong spectral lines corresponding to the primary comb, along with many spurious modes that are subjected to very large chaotic oscillations. The second route to chaos corresponds to the destabilization of solitons. Here, the unstable solitons are in a "turbulent" regime which is characterized by the pseudorandom emergence of very sharp and powerful peaks. A statistical analysis shows that these peaks which are of rare occurence and very high intensity [56] qualify as *rogue waves* [57, 58].

The chaotic spectra are prevalent in Kerr comb literature because they are relatively easy to obtain and they feature a very large spectrum (strong pump regime). However, it should be recalled that these pseudo-random spectra are nonstationary and, therefore, only partially coherent (even in the hypothetical case of a noise-free system, see ref. [59]). They are, therefore, not the most suitable combs for most applications where exceptionaly high coherence is a strong requirement.

5 Applications

5.1 Ultra-stable microwave generation

Optical frequency combs are known to be one of the most efficient technology for ultra-stable microwave generation. Traditionaly, the combs are generated using an ultra-fast mode-locked laser. Provided that they span over more than an octave, these combs can be autoreferenced, thereby allowing for the transfer of the metrological precision of optical laser frequencies down to the gigahertz or terahertz range [70]. The Nobel prize of physics has been awarded in 2005 to Theodor Hänsh and John Hall for their contributions to the optical frequency comb technique.

One of the early promise of Kerr optical frequency combs is that they could provide ultra-stable signals both in the lightwave and microwave frequency domains. Several research works have already proven that Kerr combs can effectively deliver competitive solutions for both oscillators (short-term stability) and clocks (long-term stability).

The microwaves are generated by photodetection of the output signal from the Kerr-nonlinear resonator, as shown in Fig. 7. As far as short-term stability is concerned, an early result reported a phase noise performance of −113 dBc/Hz at 10 kHz from a 22-GHz carrier, using a versatile platform that was able to provide resonators with

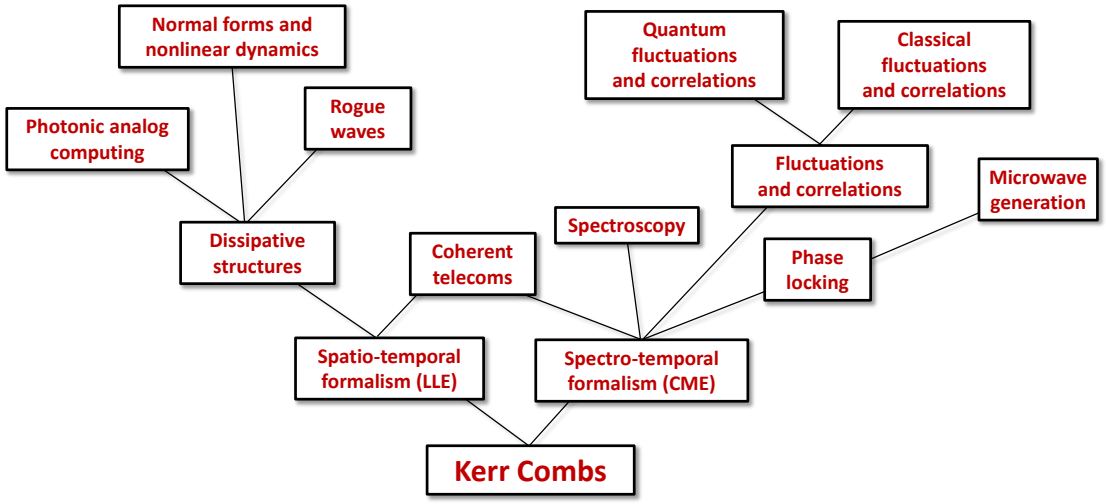

Figure 10: (Color online) Representation of some of the fundamental and applied developments related to Kerr combs. This evolutionary tree permits to visualize the cross-disciplinary nature of this topic.

Q-factors of the order of a billion at 1550 nm [60]. Miniature photonic oscillators based on Kerr combs are commercially available today with a phase noise of −115 dBc/Hz at 10 kHz offset and −130 dBc/Hz at 100 kHz offset from a 10- or 35-GHz output [61]. These performances have recently been improved with a miniature 10-GHz microwave photonic oscillator characterized by a phase noise better than −60 dBc/Hz at 10 Hz, −90 dBc/Hz at 100 Hz, and −170 dBc/Hz at 10 MHz [23]. From the perspective of long-term stability, Kerr combs with 140-GHz intermodal frequency have been stabilized with a residual one-second instability of 10^{-15}, with a microwave reference limited absolute instability of 10^{-12} [62]. Kerr combs have been successfully stabilized to atomic rubidium transitions as well [63].

It is noteworthy that Kerr combs are capabile to have a frequency span beyond one octave. For example, a Kerr frequency combs spanning from 990 to 2170 nm with a 0.85-THz FSR has been demonstrated experimentally in ref. [64]. An octave comb pumped at 1562 nm with a 128-THz span and a spacing of 226 GHz was reported in ref. [65]. Recent experiments have also shown that Kerr combs can even have a multioctave spectral span [66]. Therefore, Kerr combs can be self-referenced and be useful for metrological applications. A comprehensive analysis of noise conversion mechanisms in Kerr combs is proposed in ref. [67].

5.2 Optical coherent telecommunications

As highlighted in the previous sections, Kerr optical frequency combs are characterized by their exceptional spectral purity and coherence. They are, therefore, ideal candidates to be coherent multiwavelength emitters for ultra-high capacity optical fiber telecommunication networks, where evenly spaced and phase-locked carriers are used for the purpose of wavelength division multiplexing (WDM). These optical telecommunication networks are still in constant need for ever more transmission bandwidth, but, however, it becomes increasingly difficult and costly to generate a large number of independent and frequency-locked sub-carriers when they have to be controlled precisely and individually. Kerr combs provide a simple and cost-effective alternative technology to circumvent this drawback.

Early experiments with Kerr combs demonstrated single-channel 10 Gbit/s transmissions using an on–off keying modulation scheme [68, 69]. A leapfrog improvements was reported recently with a 1.44 Tbit/s transmission using quadrature phase shift keying with configuration where 20 channels modulated at a bitrate of 72 Gbit/s were multiplexed [59]. All the above experimental demonstrations did use Kerr combs generated with integrated RRs with million quality factor at 1550 nm. Using the experimetal setup displayed in Fig. 8, it was shown later that crystalline WGMRs with billion quality factors at 1550 nm allows to increase the transmission capacity to 144 Gbit/s per channel using a 16-quadrature amplitude modulation scheme on three multiplexed carriers [59].

5.3 Spectroscopy and mid-IR combs

Kerr optical frequency combs can be generated in a very wide range of wavelength and intermodal spacing grids. For this reason, they are considered promising tools for spectroscopic and sensing applications [71]. The overwhelming majority of Kerr combs are generated today around the telecom wavelength of 1550 nm, but the pump frequencies can be pushed downwards to 800 nm [72] and upwards to 4500 nm [73].

Naturally, the (multi-)octave spanning combs provide some of the widest frequency spans [64–66]. However, particular efforts have been invested in recent years to explore the mid-infrared (IR) range where a large set of molecules of interest have their spectroscopic signature [71]. Some of the most noticeable results along that line have been reported in refs. [73–76], where Kerr combs in the mid-IR have been successfully generated. Active research is also currently led to understand how the dispersion can be engineered in order to increase the efficiency of mid-IR comb generation [77].

5.4 Quantum applications

Kerr optical frequency combs involve interactions among individual photons and, therefore, can feature genuinely quantum properties when pumped below or above threshold as shown in Fig. 9. This quantum behavior can be understood using, for example, the QLE presented in Section 3.3.

When the system is pumped below threshold, it is classically assumed that all the sidemodes have zero power except the pumped mode. However, from the quantum viewpoint, the pump field actually interacts with the sidemodes through *spontaneous FWM*, where two pump photons of frequency $\omega_\mathrm{p} \equiv \omega_0$ are symmetrically up and down converted in the Fourier domain following $2\hbar\omega_\mathrm{p} \rightarrow \hbar\omega_\mathrm{i} + \hbar\omega_\mathrm{s}$, where $\omega_\mathrm{i} \equiv \omega_{-L}$ and $\omega_\mathrm{s} \equiv \omega_{+L}$ are the idler and signal angular frequencies, respectively (with $L > 0$). Spontaneous FWM, which is also sometimes referred to as *parametric fluorescence*, is a purely quantum phenomenon that results from the coupling between the intracavity pump photons and the vacuum fluctuations of the various sidemodes. The applications of spontaneous FWM belong to the area of quantum optics engineering, where one of the main challenge is the generation of entangled twin-photon pairs with chip-scale RRs [78–90]. These photon pairs are expected to play a key role in quantum communication protocols.

Above threshold, the photonic interaction $2\hbar\omega_\mathrm{p} \rightarrow \hbar\omega_\mathrm{i} + \hbar\omega_\mathrm{s}$ becomes stimulated instead of spontaneous, through modulational instability, for example. The semi-classical analysis (CME or LLE) predicts that the power in the sidemodes $\pm l$ is exactly the same, so that the difference $N_{\mathrm{out},\Delta} = N_{\mathrm{out},l} - N_{\mathrm{out},-l}$ of the output photon number flux is strictly null (this experimentally corresponds to the difference of optical powers photodetected for the modes $+l$ and $-l$). This situation is in contrast with the the quantum standpoint where the corresponding operator $\hat{\mathrm{N}}_{\mathrm{out},\Delta} = \hat{\mathrm{N}}_{\mathrm{out},l} - \hat{\mathrm{N}}_{\mathrm{out},-l}$ does not vanish, because there is necessarily a shot-noise floor level after any photodetection process (standard quantum noise limit). However, the system can be tuned to a quantum state where the difference in the amplitude fluctuations is *smaller* than the standard quantum noise limit, and this phenomenon corresponds to the so-called two-mode squeezing [91, 92]. This phenomenon, predicted by Lugiato and Castelli in ref. [93] for optical systems ruled by the LLE, has been experimentally observed in Kerr combs in ref. [94]. Squeezing finds its main application in ultra-high precision optical metrology.

6 Conclusion

In this review article, we have provided a general presentation of the topic of Kerr optical frequency combs. We have discussed the frameworks of analysis needed to achieve an insightful understanding of the available theoretical and experimental results in that field. We have first presented the various experimental architectures used for Kerr comb generation, with an emphasis on the generators based on crystalline and chipscale resonators. We have then introduced the two main formalisms for the theoretical understanding of Kerr combs, namely, the coupled-mode theory and the LLE. The various solutions of interest in the spatial domain have been highlighted, namely, rolls, solitons, breathers, and chaos, along with their corresponding combs in the spectral domain. We have then discussed some applications of Kerr combs with emphasis on optical communications, microwave generation, spectroscopy, and quantum applications.

Several challenges are still to be met as far as Kerr combs are concerned. For example, the nonlinear dynamics of the LLE and its bifurcation behavior is extremely rich and still deserves attention, as a full characterization of the existing stationary solutions has not been completed at this date [18, 95–97]. This nonlinear analysis is also needed in order to gain further insight in the

wide variety of phase-locking phenomena that are taking place in Kerr combs [49, 98–100] and also to optimize the Kerr comb generation process [101]. The phenomenon of the Raman scattering in ultra-high-Q resonators deserves much attention, because it arises from the same $\chi^{(3)}$ nonlinearity that is at the origin of Kerr combs. These Raman combs generally have a spectral span that is as large as few tens of terahertz and they, therefore, require to account for higher-order dispersion and nondegeneracy of spatial modes [102]. The issue of dispersion engineering is also critical, as it directly defines the spectral span of the comb [103]. Other nonlinear effects that might compete with the Kerr nonlinearity also have to be accounted for, such as Brillouin scattering [104] or even thermal effects [105]. From the application standpoint, Kerr combs can also be combined with other traditional techniques to provide a versatile set of carriers for coherent optical telecommunications [106], while the versatility of primary combs (which can permit to generate combs with an intermodal frequency higher than a terahertz) could be exploited for the purpose of terahertz generation [50]. The stochastic analysis of Kerr combs is also a topic that will probably become more prevalent at the time to evaluate the spectral purity of the lightwave [59] and microwave [67] coherent output signals, and this study will require an in-depth understanding of the noise sources in the resonators [107, 108].

The topic of Kerr combs is definitely far-reaching, interdisciplinary, and transversal from both the fundamental and applied viewpoints, as shown in Fig. 10, and we expect the forthcoming developments in this field to be of the highest relevance in many areas of contemporary science.

Acknowledgement: This work has been funded by the European Research Council (ERC) through the projects StG NextPhase and PoC Versyt, the *Centre National d'Etudes Spatiales* (CNES) through the project SHYRO, the *Région de Franche-Comté* through the project CORPS, and the Labex ACTION. The author would like to acknowledge the contribution of current and former members of his research group, namely, A. Coillet, R. Henriet, I. V. Balakireva, S. Diallo, K. Saleh, R. Marchal, R. Martinenghi, and G. Lin. He also aknowledges fruitful collaborations with several colleagues from a broad range of disciplinary areas, in particular R. Salut, C. Godey, J. Pfeifle, C. Koos, C. Finot, J.-P. Aubry, M. Haragus, J. M. Dudley, N. Yu, C. R. Menyuk, and L. Larger.

References

[1] Matsko A. B., Ilchenko V. S., Optical resonators with whispering gallery modes I: Basics, IEEE J. Sel. Top. Quantum Electron. 2006, 12, 3.

[2] Ilchenko V. S., Matsko A. B., Optical Resonators With Whispering-Gallery Modes—Part II: Applications, IEEE J. Sel. Top. Quantum Electron. 2006, 12, 15.

[3] Chiasera A., Dumeige Y., Féron P., Ferrari M., Jestin Y., Nunzi Conti G., Pelli S., Soria S., Righini G. C., Spherical whispering-gallery-mode microresonators, Laser Photon. Rev. 2010, 51, 457.

[4] Kippenberg T. J., Spillane S. M., Vahala K. J., Kerr-Nonlinearity Optical Parametric Oscillation in an Ultrahigh-Q Toroid Microcavity, Phys. Rev. Lett. 2004, 93, 083904.

[5] Savchenkov A. A., Matsko A. B., Strekalov D., Mohageg M., Ilchenko V. S., Maleki L., Low Threshold Optical Oscillations in a Whispering Gallery Mode CaF_2 Resonator, Phys. Rev. Lett. 2004, 93, 243905.

[6] Del'Haye P., Schliesser A., Arcizet A., Holzwarth R., Kippenberg T. J., Optical frequency comb generation from a monolithic microresonator, Nature 2007, 450, 1214.

[7] Kippenberg T. J., Holzwarth R., Diddams S. A., Microresonator-Based Optical Frequency Combs, Science 2011, 322, 555.

[8] Chembo Y. K., Strekalov D. V., Yu N., Spectrum and Dynamics of Optical Frequency Combs Generated with Monolithic Whispering Gallery Mode Resonators, Phys. Rev. Lett. 2010, 104, 103902.

[9] Chembo Y. K., Yu N., Modal expansion approach to optical-frequency-comb generation with monolithic whispering-gallery-mode resonators, Phys. Rev. A 2010, 82, 033801.

[10] Chembo Y. K., Yu N., On the generation of octave-spanning optical frequency combs using monolithic whispering-gallery-mode microresonators, Opt. Lett. 2010, 35, 2696.

[11] Matsko A. B., Savchenkov A. A., Maleki L., Normal group-velocity dispersion Kerr frequency comb, Opt. Lett. 2012, 37, 43.

[12] Agha I. H., Okawachi Y., Gaeta A. L., Opt. Express 2009, 17, 16209.

[13] Matsko A. B., Savchenkov A. A., Liang W., Ilchenko V. S., Seidel D., Maleki L., Mode-locked Kerr frequency combs, Opt. Lett. 2011, 36, 2845.

[14] Chembo Y. K., Menyuk C. R., Spatiotemporal Lugiato-Lefever formalism for Kerr-comb generation in whispering-gallery-mode resonators, Phys. Rev. A 2013, 87, 053852.

[15] Coen S., Randle H. G., Sylvestre T., Erkintalo M., Modeling of octave-spanning Kerr frequency combs using a generalized mean-field Lugiato-Lefever model, Opt. Lett. 2013, 38, 37.

[16] Lugiato L. A., Lefever R., Spatial Dissipative Structures in Passive Optical Systems, Phys. Rev. Lett. 1987, 58, 2209.

[17] Coillet A., Balakireva I., Henriet R., Saleh K., Larger L., Dudley J. M., Menyuk C. R., Chembo Y. K., Azimuthal Turing Patterns, Bright and Dark Cavity Solitons in Kerr Combs generated with Whispering-Gallery Mode Resonators, IEEE Photonics Journal 2013, 5, 6100409.

[18] Godey C., Balakireva I. V., Coillet A., Chembo Y. K., Stability analysis of the spatiotemporal Lugiato-Lefever model for Kerr optical frequency combs in the anomalous and normal dispersion regimes, Phys. Rev. A. 2014, 89, 063814.

[19] Parra-Rivas P., Gomila D., Matias M. A., Coen S., Gelens L., Dynamics of localized and patterned structures in the Lugiato-Lefever equation determine the stability and shape of optical frequency combs, Phys. Rev. A. 2014, 89, 043813.
[20] Levy J. S., Gondarenko A., Foster M. A., Turner-Foster A. C., Gaeta A. L., Lipson M., CMOS-compatible multiple-wavelength oscillator for on-chip optical interconnects, Nature Photonics 2010, 4, 37.
[21] Ferdous F., Miao H., Leaird D. E., Srinivasan K., Wang J., Chen L., Varghese L. T., Weiner A. M., Spectral line-by-line pulse shaping of on-chip microresonator frequency combs, Nature Photonics 2011, 5, 770.
[22] Moss D. J., Morandotti R., Gaeta A. L., Lipson M., New CMOS-compatible platforms based on silicon nitride and Hydex for nonlinear optics, Nature Photonics 2013, 7, 597.
[23] Liang W., Eliyahu D., Ilchenko V. S., Savchenkov A. A., Matsko A. B., Seidel D., Maleki L., High spectral purity Kerr frequency comb radio frequency photonic oscillator, Nature Communications 2015, 6, 7957.
[24] Savchenkov A. A., Matsko A. B., Ilchenko V. S., Maleki L., Optical resonators with ten million finesse, Opt. Express 2007, 115, 6768.
[25] Grudinin I. S., Yu N., Maleki L., Generation of optical frequency combs with a CaF_2 resonator, Opt. Lett. 2009, 34, 878–880.
[26] Sprenger B., Schwefel H. G. L., Lu Z. H., Svitlov S., Wang, L. J., CaF_2 whispering-gallery-mode-resonator stabilized-narrow-linewidth laser, Opt. Lett. 2010, 35, 2870–2872
[27] Tavernier H., Salzenstein P., Volyanskiy K., Chembo Y. K., Larger L., Magnesium Fluoride Whispering Gallery Mode Disk-Resonators for Microwave Photonics Applications, IEEE Phot. Tech. Lett. 2010, 22, 1629–1631.
[28] Liang W., Savchenkov A. A., Matsko A. B., Ilchenko V. S., Seidel D., Maleki L., Generation of near-infrared frequency combs from a MgF_2 whispering gallery mode resonator, Opt. Lett. 2011, 36, 2290.
[29] Henriet R., Coillet A., Saleh K., Larger L., Chembo Y. K., Barium fluoride and lithium fluoride whispering-gallery mode resonators for photonics applications, Opt. Eng. 2014, 53, 071821.
[30] Lin G., Diallo S., Henriet R., Jacquot M., Chembo Y. K., Barium fluoride whispering-gallery-mode disk-resonator with one billion quality-factor, Opt. Lett. 2014, 39, 6009.
[31] Henriet R., Lin G., Coillet A., Jacquot M., Furfaro L., Larger L., Chembo Y. K. Kerr optical frequency comb generation in strontium fluoride whispering-gallery mode resonators with billion quality factor, Opt. Lett. 2015, 40, 1567.
[32] Volyanskiy K., Salzenstein P., Tavernier H., Pogurmirskiy M., Chembo Y. K., Larger L., Compact optoelectronic microwave oscillators using ultra-high Q whispering gallery mode disk-resonators and phase modulation, Opt. Express. 2010, 18, 22358–22363.
[33] Papp S. B., Diddams S. A. Spectral and temporal characterization of a fused-quartz-microresonator optical frequency comb. Phys. Rev. A 2011, 84, 053833.
[34] Ilchenko V. S., Savchenkov A. A., Byrd J., Solomatine I., Matsko A. B., Seidel D., Maleki L., Crystal quartz optical whispering-gallery resonators, Opt. Lett. 2008, 33, 1569–1571.
[35] Hausmann B. J. M., Bulu I., Venkataraman V., Deotare P., Loncar M., Diamond nonlinear photonics, Nature Photonics 2014, 8, 369–374.
[36] Coillet A., Henriet R., Huy K. P., Jacquot M., Furfaro L., Balakireva I., Larger L., Chembo Y. K., Microwave Photonics Systems Based on Whispering-gallery-mode Resonators, J. Vis. Exp. 2013, 78, e50423.
[37] Papp S. B., Del'Haye P., Diddams S. A., Mechanical Control of a Microrod-Resonator Optical Frequency Comb, Phys. Rev. X. 2013, 3, 031003.
[38] Maleki L., The optoelectronic oscillator, Nature Photonics 2011, 5, 728.
[39] Dumeige Y., Trebaol S., Ghisa L., Nguyen T. K. N., Tavernier H., Féron P., Determination of coupling regime of high-Q resonators and optical gain of highly selective amplifiers, J. Opt. Soc. Am. B 2008, 25, 2073.
[40] Coillet A., Henriet R., Salzenstein P., Phan Huy K., Larger L., Chembo Y. K., Time-domain Dynamics and Stability Analysis of Optoelectronic Oscillators based on Whispering-Gallery Mode Resonators, IEEE J. Sel. Top. Quantum Electron. 2013, 19, 6000112.
[41] Saleh K., Lin G., Chembo Y. K., Effect of Laser Coupling and Active Stabilization on the Phase Noise Performance of Optoelectronic Microwave Oscillators Based on Whispering-Gallery-Mode Resonators, IEEE Phot. J. 2015, 7, 5500111.
[42] Saleh K., Henriet R., Diallo S., Lin G., Martinenghi R., Balakireva I. V., Salzenstein P., Coillet A., Chembo Y. K., Phase noise performance comparison between optoelectronic oscillators based on optical delay lines and whispering gallery mode resonators, Opt. Express 2014, 22, 32158–32173
[43] Agrawal G. P., Nonlinear Fiber Optics, Fifth Edition, Academic Press (2013).
[44] Haelterman M., Trillo S., Wabnitz S., Additive-modulation-instability ring laser in the normal dispersion regime of a fiber Opt. Lett. 1992, 17, 745.
[45] Leo F., Coen S., Kockaert P., Gorza S.-P., Emplit P., Haelterman M., Temporal cavity solitons in one-dimensional Kerr media as bits in an all-optical buffer, Nature Photonics 2010 4, 471.
[46] Chembo Y. K., Quantum Dynamics of Kerr Optical Frequency Combs below and above Threshold: Spontaneous Four-Wave-Mixing, Entanglement and Squeezed States of Light, arXiv:1412.5700v2 [quant-ph], 2015.
[47] Hansson T., Modotto D., Wabnitz S., Dynamics of the modulational instability in microresonator frequency combs, Phys. Rev. A 2013, 88, 023819.
[48] Turing A. M., The Chemical Basis of Morphogenesis, Phil. Trans. of the R. Soc. Ser. B 1952, 237, 37.
[49] Coillet A. and Chembo Y. K., On the robustness of phase locking in Kerr optical frequency combs, Opt. Lett. 2014, 39, 1529.
[50] Lin G., Saleh K., Henriet R., Diallo S., Martinenghi R., Coillet A., Chembo Y. K., Wide-range tunability, thermal locking, and mode-crossing effects in Kerr optical frequency combs, Opt. Eng. 2014, 53, 122602.
[51] Herr T., Brasch V., Jost J. D., Wang C. Y., Kondratiev N. M., Gorodetsky M. L., Kippenberg T. J., Temporal solitons in optical microresonators, Nature Photon. 2014, 8, 145.
[52] Taheri H., Eftekhar A. A., Wiesenfeld K., Adibi A., Soliton Formation in Whispering-Gallery-Mode Resonators via Input Phase Modulation, IEEE Phot. J. 2015, 7, 2200309.
[53] Lobanov V. E., Lihachev G., Kippenberg T. J., Gorodetsky M. L., Frequency combs and platicons in optical microresonators with normal GVD, Opt. Express 2015, 23, 7713.

[54] Matsko A. B., Liang W., Savchenkov A. A., Maleki L., Chaotic dynamics of frequency combs generated with continuously pumped nonlinear microresonators, Opt. Lett. 2013, 38, 525.
[55] A. Coillet and Y. K. Chembo, Routes to spatiotemporal chaos in Kerr optical frequency combs, Chaos **24**, 013313 (2014).
[56] Coillet A., Dudley J., Genty G., Larger L., Chembo Y. K., Optical Rogue Waves in Whispering-Gallery-Mode Resonators, Phys. Rev. A 2014, 89, 013835.
[57] Akhmediev N., Pelinovsky E., Editors, Rogue waves - Towards a unifying concept, Special issue of the Eur. Phys. J. Spe. Top., 2010.
[58] Akhmediev N., Dudley J. M., Solli D. R., Turitsyn S. K., Recent progress in investigating optical rogue waves, J. Opt. 2013, 15, 060201.
[59] Pfeifle J., Coillet A., Henriet R., Saleh K., Schindler P., Weimann C., Freude W., Balakireva I. V., Larger L., Koos C., Chembo Y. K., Optimally Coherent Kerr Combs Generated with Crystalline Whispering Gallery Mode Resonators for Ultrahigh Capacity Fiber Communications, Phys. Rev. Lett. 2015, 114, 093902.
[60] Li J., Lee H., Chen T., Vahala K. J., Low-Pump-Power, Low-Phase-Noise, and Microwave to Millimeter-Wave Repetition Rate Operation in Microcombs, Phys. Rev. Lett. 2012, 109, 233901.
[61] Savchenkov A. A., Eliyahu D., Liang W., Ilchenko V. S., Byrd J., Matsko A. B., Seidel D., Maleki L., Stabilization of a Kerr frequency comb oscillator, Opt. Lett. 2013, 38, 2636.
[62] Del'Haye P., Papp S. B., Diddams S. A., Hybrid Electro-Optically Modulated Microcombs, Phys. Rev. Lett. 2012, 109, 263901.
[63] Papp S. B., Beha K., Del'Haye P., Quinlan F., Lee H., Vahala K. J., Diddams S. A., Microresonator frequency comb optical clock, Optica 2014, 1, 10.
[64] Del'Haye P., Herr T., Gavartin E., Gorodetsky M.L., Holzwarth R., Kippenberg T.J., Octave Spanning Tunable Frequency Comb from a Microresonator, Phys. Rev. Lett. 2011, 107, 63901.
[65] Okawachi Y., Saha K., Levy J. S., Wen Y. H., Lipson M., Gaeta A. L., Octave-spanning frequency comb generation in a silicon nitride chip, Opt. Lett. 2011, 36, 3398.
[66] Liang W., Savchenkov A. A., Xie Z., McMillan J. F., Burkhart J., Ilchenko V. S., Wong C. W., Matsko A. B., Maleki L., Miniature multioctave light source based on a monolithic microcavity, Optica 2015, 2, 40.
[67] Matsko A. B., Maleki L., Noise conversion in Kerr comb RF photonic oscillators, J. Opt. Soc. Am. B 2015, 32, 232.
[68] Wang P.-H., Ferdous F., Miao H., Wang J., Leaird D. E., Srinivasan K., Chen L., Aksyuk V., Weiner A. M., Observation of correlation between route to formation, coherence, noise, and communication performance of Kerr combs, Opt. Express 2012, 20, 29284.
[69] Levy J., Saha K., Okawachi Y., Foster M., Gaeta A., Lipson M., High-performance silicon-nitride-based multiple-wavelength source, IEEE Phot. Tech. Lett. 2012, 24, 1375.
[70] T. W. Hansch, Nobel Lecture: Passion for precision, Rev. Mod. Phys. 2006, 78, 1297.
[71] Schliesser A., Picqué N., Hänsch T. W., Mid-infrared frequency combs, Nature Photonics 2012, 6, 440.
[72] Savchenkov A. A., Matsko A. B., Liang W., Ilchenko V. S., Seidel D., Maleki L., Kerr combs with selectable central frequency, Nature Photonics 2011, 5, 293.
[73] Savchenkov A. A., Ilchenko V. S., Di Teodoro F., Belden P. M., Lotshaw W. T., Matsko A. B., Maleki L., Generation of Kerr combs centered at $4.5\ \mu$m in crystalline microresonators pumped with quantum-cascade lasers, Opt. Lett 2015, 40, 3468.
[74] Wang C. Y., Herr T., Del'Haye P., Schliesser A., Hofer J., Holzwarth R., Hänsch T. W., Picqué N., Kippenberg, T. J., Mid-infrared optical frequency combs at $2.5\ \mu$m based on crystalline microresonators, Nature Communications 2013, 4, 1345.
[75] Griffith A. G., Lau R. K. W., Cardenas J., Okawachi Y., Mohanty A. , Fain R., Lee Y. H. D., Yu M., Phare C. T., Poitras C. B., Gaeta A. L., Lipson M., Silicon-chip mid-infrared frequency comb generation, Nature Communications 2015, 6, 6299.
[76] Lecaplain C., Javerzac-Galy C., Lucas E., Jost J. D., Kippenberg T. J., Quantum cascade laser Kerr frequency comb, arXiv:1506.00626, 2015.
[77] Lin G., Chembo Y. K., On the dispersion management of fluorite whispering-gallery mode resonators for Kerr optical frequency comb generation in the telecom and mid-infrared range, Opt. Express 2015, 23, 1594–1604.
[78] Sharping J. E., Lee K. F., Foster M. A., Turner A. C., Schmidt B. S., Lipson M., Gaeta A. L., Kumar P., Generation of correlated photons in nanoscale silicon waveguides, Optics Express 2006, 14, 12388.
[79] Clemmen S., Phan-Huy K., Bogaerts W., Baets R. G., Emplit Ph., Massar S., Continuous wave photon pair generation in silicon-on-insulator waveguides and ring resonators, Opt. Express 2009, 17, 16558.
[80] Helt L. G., Yang Z., Liscidini M., Sipe J. E., Spontaneous four-wave mixing in microring resonators, Opt. Lett. 2010, 35, 3006.
[81] Chen J., Levine Z. H., Fan J., Migdall A. L., Frequency-bin entangled comb of photon pairs from a Silicon-on-Insulator microresonator, Opt. Express 2011, 19, 1470.
[82] Azzini S., Grassani D., Strain M. J., Sorel M., Helt L. G., Sipe J. E., Liscidini M., Galli M., Bajoni D., Ultra-low power generation of twin photons in a compact silicon ring resonator, Opt. Express 2012, 20, 23100.
[83] Helt L. G., Liscidini M., Sipe J. E., How does it scale? Comparing quantum and classical nonlinear optical processes in integrated devices, J. Opt. Soc. Am. 2012, 29, 2199.
[84] Azzini S., Grassani D., Galli M., Andreani L. C., Sorel M., Strain M. J., Helt L. G., Sipe J. E., Liscidini M., Bajoni D., From classical four-wave mixing to parametric fluorescence in silicon microring resonators, Opt. Express 2012, 37, 3807.
[85] Camacho R. M., Entangled photon generation using four-wave mixing in azimuthally symmetric microresonators, Opt. Express 2012, 20, 21977.
[86] Matsuda N., Le Jeannic H., Fukuda H., Tsuchizawa T., Munro W. J., Shimizu K., Yamada K., Tokura Y., Takesue H., A monolithically integrated polarization entangled photon pair source on a silicon chip, Sci. Rep. 2012, 2, 817.
[87] Engin E., Bonneau D., Natarajan C. M., Clark A. S., Tanner M. G., Hadfield R. H., Dorenbos S. N., Zwiller V., Ohira K., Suzuki N., Yoshida H., Iizuka N., Ezaki M., O'Brien J. L., Thompson M. G., Photon pair generation in a silicon micro-ring resonator with reverse bias enhancement, Opt. Express 2013, 21, 27826.
[88] Reimer C., Caspani L., Clerici M., Ferrera M., Kues M., Peccianti M., Pasquazi A., Razzari L., Little B. E., Chu S. T., Moss D. J., Morandotti R., Integrated frequency comb source of heralded single photons, Opt. Express 2014, 22, 6535.
[89] Vernon Z., Sipe J. E., Spontaneous four-wave mixing in lossy microring resonators, arXiv:1502.05900 [quant-ph], 2015.
[90] Grassani D., Azzini S., Liscidini M., Galli M., Strain M. J., Sorel M., Sipe J. E., Bajoni D., Micrometer-scale integrated silicon source of time-energy entangled photons, Optica 2015, 2, 88.

[91] Fabre C., Squeezed states of light, Phys. Rep. 1992, 19, 215.
[92] Sanders B. C., Review of coherent entangled states, J. Phys. A: Math. Theor. 2012, 45, 244002.
[93] Lugiato L. A., Castelli F., Quantum Noise Reduction in a Spatial Dissipative Structure, Phys. Rev. Lett., 1992, 68, 3284.
[94] Dutt A., Luke K., Manipatruni S., Gaeta A. L., Nussenzveig P., Lipson M., On-Chip Optical Squeezing, Phys. Rev. Applied 2015, 3, 044005.
[95] Haragus M., Iooss G., Local Bifurcations, Center Manifolds, and Normal Forms in Infinite-Dimensional Dynamical Systems, Springer, 2010.
[96] Miyaji T., Ohnishi I., Tsutsumi Y., Bifurcation analysis to the Lugiato–Lefever equation in one space dimension, Physica D 2010, 239, 2066.
[97] Kozyreff G., Localized Turing patterns in nonlinear optical cavities, Physica D 2012, 241, 936.
[98] Herr T., Hartinger K., Riemensberger J., Wang C. Y., Gavartin E., Holzwarth R., Gorodetsky M. L., Kippenberg T. J., Universal formation dynamics and noise of Kerr-frequency combs in microresonators Nature Photonics, 2012, 6, 480.
[99] Del'Haye P., Beha K., Papp S. B., Diddams S. A., Self-Injection Locking and Phase-Locked States in Microresonator-Based Optical Frequency Combs, Phys. Rev. Lett. 2014, 112, 043905.
[100] Del'Haye P., Coillet A., Loh W., Beha K., Papp S. B., Diddams S. A., Phase steps and resonator detuning measurements in microresonator frequency combs, Nature Communications 2015, 6, 5668.
[101] Bao C., Zhang L., Matsko A., Nonlinear conversion efficiency in Kerr frequency comb generation, Opt. Lett. 2014, 39, 6126.
[102] Chembo Y. K., Grudinin I. S., Yu N., Spatiotemporal dynamics of Kerr-Raman optical frequency combs, Phys. Rev. A 2015, 92, 043818.
[103] Grudinin I. S., Yu N., Dispersion engineering of crystalline resonators via microstructuring, Optica 2015, 2, 221.
[104] Lin G., Diallo S., Saleh K., Martinenghi R., Beugnot J.-C., Sylvestre T., Chembo Y. K., Cascaded Brillouin lasing in monolithic barium fluoride whispering gallery mode resonators, Appl. Phys. Lett. 2014, 105, 231103.
[105] Diallo S., Lin G., Chembo Y. K., Giant thermo-optical relaxation oscillations in millimeter-size whispering gallery mode disk resonators, Opt. Lett. 2015, 40, 3834.
[106] Lin G., Martinenghi R., Diallo S., Saleh K., Coillet A., Chembo Y. K., Spectro-temporal dynamics of Kerr combs with parametric seeding Appl. Opt. 2015, 54, 2407.
[107] Matsko A. B., Savchenkov A. A., Yu N., Maleki L., Whispering-gallery-mode resonators as frequency references. I. Fundamental limitations, J. Opt. Soc. Am. B 2007, 24, 1324.
[108] Savchenkov A. A., Matsko A. B., Ilchenko V. S., Yu N., Maleki L., Whispering-gallery-mode resonators as frequency references. II. Stabilization, J. Opt. Soc. Am. B 2007, 24, 2988.